Published in final edited form as:
Curr Biol. 2012 January 24; 22(2): 103–112. doi:10.1016/j.cub.2011.12.015.

The HSF-like Transcription Factor TBF1 Is a Major Molecular Switch for Plant Growth-to-Defense Transition

Karolina M. Pajerowska-Mukhtar[1,5], **Wei Wang**[1], **Yasuomi Tada**[2], **Nodoka Oka**[3], **Chandra L. Tucker**[1,6], **Jose Pedro Fonseca**[1], and **Xinnian Dong**[1,4,*]

[1]Department of Biology, Box 90338, Duke University, Durham, NC 27708, USA

[2]Life Science Research Center, Institute of Research Promotion, Kagawa University, 2393 Ikenobe, Miki-cho, Kita-gun, Kagawa 761-0795, Japan

[3]Faculty of Agriculture, Kagawa University, 2393 Ikenobe, Miki-cho, Kita-gun, Kagawa 761-0795, Japan

[4]Howard Hughes Medical Institute, Duke University, Durham, NC 27708, USA

Summary

Background—Induction of plant immune responses involves significant transcription reprogramming that prioritizes defense over growth-related cellular functions. Despite intensive forward genetic screens and genome-wide expression-profiling studies, a limited number of transcription factors have been found that regulate this transition.

Results—Using the endoplasmic-reticulum-resident genes required for antimicrobial protein secretion as markers, we identified a heat-shock factor-like transcription factor that specifically binds to the *TL1* (GAAGAAGAA) *cis* element required for the induction of these genes. Surprisingly, plants lacking this *TL1*-binding factor, TBF1, respond normally to heat stress but are compromised in immune responses induced by salicylic acid and by microbe-associated molecular pattern, elf18. Genome-wide expression profiling indicates that TBF1 plays a key role in the growth-to-defense transition. Moreover, the expression of *TBF1* itself is tightly regulated at both the transcriptional and translational levels. Two upstream open reading frames encoding multiple aromatic amino acids were found 5′ of the translation initiation codon of TBF1 and shown to affect its translation.

Conclusions—Through this unique regulatory mechanism, TBF1 can sense the metabolic changes upon pathogen invasion and trigger the specific transcriptional reprogramming through its target genes expression.

*Correspondence: xdong@duke.edu.
[5]Current address: Department of Biology, University of Alabama at Birmingham, Campbell Hall 369, 1300 University Boulevard, Birmingham, AL 35294, USA
[6]Current Address: Department of Pharmacology, University of Colorado School of Medicine, Mail Stop 8303, Box 6511, Aurora, CO 80045, USA

Accession Numbers

The microarray data reported in this paper have been deposited in the Gene Expression Omnibus (GEO) database under the accession number GSE34047.

Supplemental Information

Supplemental Information includes five figures, three tables, and Supplemental Experimental Procedures and can be found with this article online at doi:10.1016/j.cub.2011.12.015.

Introduction

The sessile nature of plants subjects them to constant biotic and abiotic stresses. Even though plants do not have specialized immune cells, they can mount both local and systemic immune responses [1]. This requires extensive cross-talk between plant defense and other physiological processes. Induction of defense responses involves the recognition of microbe-associated molecular patterns (MAMPs) by membrane-associated receptors leading to MAMP-triggered immunity (MTI) and of pathogen-delivered effectors by cytosolic receptors resulting in effector-triggered immunity (ETI) [2]. Besides these local defense mechanisms, salicylic acid (SA) is produced during local infection that can lead to systemic acquired resistance (SAR). In *Arabidopsis*, SA signals through the key immune regulator NPR1 (nonexpressor of *PR* genes), which is required for subsequent transcriptional changes of as many as ~10% of all genes [3]. However, unlike the signal-specific MTI and ETI, SAR is broad spectrum and long lasting [4].

SAR-associated transcriptional reprogramming redirects cellular resources, normally dedicated to growth-related activities, toward de novo synthesis of antimicrobial proteins such as the pathogenesis-related (PR) proteins. Prior to PR protein accumulation, endoplasmic reticulum (ER)-resident genes encoding the secretory pathway machinery are coordinately upregulated to ensure efficient posttranslational modification and secretion of these antimicrobial peptides [3, 5]. The involvement of the ER function is not restricted to SAR. A connection between the ER-resident genes and MTI has been revealed in studies demonstrating that the biogenesis of EFR, a membrane-bound receptor for the MAMP signal elf18 (the N-terminal 18 amino acids of the bacterial translation elongation factor Tu, EF-Tu), requires the *N*-glycosylation pathway genes encoding the calreticulin 3 (*CRT3*) and the UDP-glucose:glycoprotein glycosyltransferase *STT3A* in the ER quality control mechanism (ERQC) [6, 7].

Previously, we showed that induction of both *PR* and ER-resident genes requires the transcription cofactor NPR1. Upon SA induction, NPR1 is nuclear translocated [8] and induces *PR* genes through its interaction with the TGA transcription factors (TFs) at *PR* genes promoters [9, 10]. However, it is not known how NPR1 regulates the ER-resident genes. TGA TFs are unlikely candidates, because in the *tga* mutants, expression of ER-resident genes is unaltered following induction [3]. Significant enrichment of a novel *cis* element *TL1* (translocon 1; *GAAGAAGAA*) in the promoter regions of these NPR1-dependent ER-resident genes suggests the involvement of an unknown TF [3]. Point mutations in the *TL1* elements of the *BiP2* (*Lumenal Binding Protein 2*) promoter abolished the inducibility of this gene upon SA treatment [3]. Because the secretory pathway is required not only for defense but also for many other cellular functions, identification of this *TL1*-binding TF is vital to our understanding of the mechanism controlling the growth-to-defense transition.

Here, we report the identification of a heat-shock factor-like protein (HSF4/HsfB1) that binds to the *TL1 cis* element and regulates the expression of genes containing this element in their promoters. Because mutants of this TF have normal heat-shock responses but are compromised in the growth-to-defense transition upon pathogen challenge, we renamed it the *TL1*-binding transcription factor 1, or TBF1. Consistent with its key role in this general control, the translation of TBF1 is tightly regulated through two upstream open reading frames (uORFs) enriched in aromatic amino acids, which are precursors of a large array of plant secondary metabolites involved in defense.

Results

TBF1 Is a TF that Binds to the *TL1 cis* Element Enriched in Defense-Related Gene Promoters

The *TL1 cis* element (consensus sequence *GAAGAAGAA*) in the ER-resident genes is essential for their activation in response to SA induction [3]. We examined publically available microarray data (see Supplemental Information available online) and found that the *TL1 cis* element is enriched in promoters of genes regulated by elf26 (the first 26 amino acids of EF-Tu) ($p < 0.001$) and flg22 ($p < 0.01$), indicating that this novel element may play a role in MTI. Interestingly, we detected no significant enrichment of *TL1* when all of the BTH (benzothiadiazole; an SA analog)-affected promoters were analyzed even though the element was first discovered in the SA-induced, NPR1-dependent ER-resident genes [3].

Next, we searched the TF that binds to *TL1* using the TFSEARCH database and found HSFs of *Saccharomyces cerevisiae* and *Drosophila melanogaster* as potential candidates. The *Arabidopsis* genome contains 21 *HSF*-like genes. Several reports have indicated the involvement of the HSFs in immediate heat response, acquired thermotolerance, sensing of reactive oxygen species (ROS), and seed development [11, 12]. To identify a candidate gene for *TBF1*, we first examined publically available expression data for profiles of the *Arabidopsis HSF* family members (see Supplemental Information). Only one gene family member, *HSF4* (also known as *HsfB1*; At4g36990), was strongly induced by BTH as well as virulent and avirulent *Pseudomonas syringae* pv. *maculicola* (*Psm*) ES4326 bacteria. Because *Arabidopsis HSF4* and its tomato homolog do not functionally complement the yeast *hsf1* mutant strain [13] (Daniel Neef and Dennis Thiele, personal communication) and its overexpression has little effect on heat-shock protein expression or thermotolerance [14, 15], we speculated that *HSF4* does not encode a typical heat-shock factor. Its pathogen-inducible expression pattern suggests that it has a novel function related to plant immunity and is a candidate for TBF1.

In the current study, we demonstrated HSF4 to be the *TL1*-binding TF (TBF1) through a yeast one-hybrid (Y1H) assay in which the fragment of *BiP2* promoter containing multiple functional *TL1 cis*-elements [3] was used as bait. We constructed two yeast bait strains containing the wild-type (WT) and the mutant (*mTL1*) *BiP2* promoters, respectively (Figures S1A and S1B). Expression of TBF1-AD (activation domain) in Strain 1 activated both *HIS3* and *LacZ* reporters driven by the WT *BiP2* promoter (Figures 1A and 1B). The binding specificity of TBF1 to *TL1* was confirmed in Strain 2 where the two single nucleotide substitutions in the *mTL1* core binding sequence blocked the induction of *LacZ*, whereas the control *HIS3* reporter with the WT *TL1* was induced normally (Figure 1B).

TBF1 binding to the *TL1 cis* element was further demonstrated by electrophoretic mobility shift assay using protein extracts from WT and an insertional knock-out *TBF1* mutant, *tbf1* (Figures S1C and S1D). WT displayed an upshifted band whose intensity was further enhanced in the extract made from plants treated with SA (Figure 1C). This band was diminished in the *tbf1* mutant extract, indicating that TBF1 is required for the DNA-protein complex formation. Competition assay using nonradioactive *TL1* and mutant *mTL1* probes indicated that the observed TBF1 binding was specific to the *TL1* consensus sequence.

To test TBF1 DNA-binding activity in vivo, we generated transgenic *tbf1* plants expressing a translational fusion between *TBF1* and *GFP* driven by the endogenous *TBF1* promoter (*TBF1p:TBF1-GFP*). Because the fusion protein was proven to be biologically active through genetic complementation of the *tbf1* mutant phenotype (Figure S1E), we used it for chromatin immunoprecipitation (ChIP). As shown in Figure 1D, using six pairs of primers spanning different regions of the *BiP2* promoter, we detected sequence enrichment

corresponding to the *TL1*-containing region 2 in both uninduced and SA-treated samples, region 3 in the SA-treated sample, and region 4 in the uninduced sample. No enrichment was found in regions 1, 5, and 6 that do not contain the *TL1* element.

TBF1 Is a Major Molecular Switch Involved in Transcriptional Reprogramming Induced by SA and elf18

In the test for TBF1 dependency, we found that the induction of *BiP2* and *CRT3*, whose promoters contain multiple copies of *TL1* elements, was compromised in the *tbf1* mutant and in *npr1-1* (Figure 2A). Consequently, the BiP2 protein accumulation was inhibited in the SA-treated *tbf1* mutant plants (Figure S2A). In contrast, induction of two other ER-resident genes, *BiP3* and *CRT1*, which do not have *TL1* in their promoters, was not affected in *tbf1* (Figure 2B), confirming the specificity of TBF1 to *TL1*.

We next performed a genome-wide transcriptional profiling on WT and *tbf1* plants upon SA and elf18 treatments to determine the global effect of TBF1. We found 1,269 and 1,792 TBF1-dependent genes differentially regulated by SA and elf18, respectively ($p < 0.05$, fold change > 2). However, only ~8% of these genes were regulated by both signals (Figure 2C; Table S1), indicating that TBF1 controls distinct output genes in SAR and MTI. Moreover, the total numbers of significantly induced and repressed genes (the top heatmaps in Figures 2D and 2E), the degrees of TBF1 dependency (the middle heatmaps), and the numbers of *TL1 cis* elements present in the gene promoters (the bottom heatmaps) indicate that TBF1 plays a greater role in SA- and elf18-mediated transcription repression than in induction. This finding is in agreement with the previous work indicating that class B-Hsfs mainly act as repressors of target gene expression [16, 17].

Gene ontology (GO) analysis identified a significantly enriched cluster of SA-induced secretory pathway genes ($p \leq 0.001$; Figure 2D "membrane proteins," Table S1), recapitulating our earlier findings [3]. In addition, we identified several major SA- and elf18-mediated and TBF1-dependent functional categories including genes known to encode defense-related proteins, ribosomal proteins, chloroplast function-related proteins, and abiotic stress signal transducers (Figures 2D and 2E; Table S1; described in more detail in Supplemental Information) [18]. We postulate that these genes are likely directly controlled by TBF1 because their regulatory regions contain the *TL1* element (Table S1).

Expression changes observed in the microarray experiment were further confirmed through qRT-PCR of independent biological samples on 26 selected genes representing various GO categories listed in Figures 2D and 2E (Figures S2B–S2E).

TBF1 Plays a Key Role in the Growth-to-Defense Transition

Upon SA treatment, TBF1 downregulates genes encoding chloroplast proteins (Figure 2D) —an effect that is known to be associated with SA [19]. Interestingly, chloroplast function-related genes were even more profoundly repressed by elf18 (Figure 2E), indicating that TBF1 might play a general role as a major molecular switch in the growth-to-defense transition. To test this, we first measured the growth of both WT and the *tbf1* mutant plants. As shown in Figure 3A, in the absence of SA or elf18, the *tbf1* mutant grew at a similar rate as WT. In the presence of elf18 or increasing SA concentrations, however, the growth of the WT plants was significantly inhibited. This effect was partially alleviated in the *tbf1* mutant. In contrast, another MAMP signal, flg22, exerted a similar growth-suppressing effect on both WT and *tbf1* seedlings (Figure S3A).

We performed an additional series of tests to determine the stress responses mediated by TBF1. Even though the *tbf1* mutant has been shown to have normal heat-induced marker gene expression (Figure S3B) and plays no detectable role in the heat-shock response [20],

its defect in the induction of multiple chaperone genes prompted us to examine the unfolded protein response (UPR). When the plants were treated with the UPR inducer tunicamycin, seedling survival rate for *tbf1* was only ~20% compared to ~60% for WT (Figure 3B), indicating that TBF1 plays a role in UPR.

The capacity of TBF1 to efficiently secrete antimicrobial PR1 protein was evaluated next. Whereas the *PR1* transcript induction and total PR1 protein levels were unchanged in *tbf1* (Figure 3C; Figure S3C), secreted PR1 in the intercellular wash fluid was dramatically reduced in the *tbf1* mutant, as in the control *bip2 dad1* double mutant [3], compared to WT. This phenotype was complemented in the transgenic line carrying a genomic fragment encompassing upstream regulatory sequences (3,554 bp) and the coding region (1,047 bp) of *TBF1* (TBF1 complementation). The defect in secretion of anti-microbial proteins in the *tbf1* mutant correlated with more than 1 log higher growth of the bacterial pathogen *Psm* ES4326 compared to WT and the complementation line (Figure 3D). In response to SA induction, less than 1 log reduction in *Psm* ES4326 growth was observed in the *tbf1* mutant as opposed to the ~2 log reduction detected in the WT plants (Figure 3E). SA-inducible defenses were restored in the TBF1 complementation line, whereas *npr1-1* was completely deficient in establishing resistance.

We next examined whether the *tbf1* mutant is capable of mounting effective MTI using elf18 and flg22. WT plants pre-treated with either signal showed a more than 1 log reduction in *Psm* ES4326 growth compared to mock-treated samples (Figure 3F; Figure S3D). The *tbf1* mutant, on the other hand, completely failed to establish the resistance induced by elf18. Interestingly, this defect is specific to elf18 because flg22-induced resistance was intact in the *tbf1* mutant (Figures S3D and S3E). Although previous studies showed that flg22 and elf18 induce largely overlapping sets of genes [21], our results, however, are consistent with the genetic data showing that the perception of elf18, but not flg22, specifically requires the ERQC mechanism [6, 7, 22, 23] and with the fact that TBF1 controls the induction of these ERQC genes (Figure 2A). The molecular mechanism underlying this TBF1 requirement has yet to be determined.

Another observation from the *Psm* ES4326 infection experiment was the near-normal response to elf18 observed in the SA-insensitive *npr1-1* mutant (Figure 3F). Even though there was an overall increase in *Psm* ES4326 growth in *npr1-1*, elf18 pretreatment could still result in a more than 1 log reduction in pathogen growth similar to that observed in the WT. This result is in accordance with the expression profiling data showing that elf18 and SA induce distinct sets of genes (Figure 2C). Moreover, a recently published study demonstrated that MTI induced by flg22 and elf18 is largely intact in the *sid2* mutant, which is deficient in SA synthesis [24]. MTI and SAR are two temporally and spatially separate immune responses. The former occurs locally and immediately upon pathogen challenge, whereas the latter is a systemic response induced after the local response.

Translation of TBF1 Is Controlled by uORFs Sensitive to Cellular Metabolic Changes

Our expression profiling and genetic data show that TBF1 is a major molecular switch that, upon pathogen challenge, turns on multiple defenses and inhibits primary growth and development (Figures 2 and 3). To understand how TBF1 itself is regulated, we analyzed its expression patterns upon SA treatment and detected the maximum accumulation of TBF1 transcript 4 hr after the treatment (Figure 4A). We further demonstrated that functional NPR1 is required for SA-mediated *TBF1* transcription. Interestingly, TBF1 also plays a role in regulating *NPR1* as the *NPR1* transcript levels were diminished in *tbf1* (Figure 4B), suggesting a feedback mechanism between these two key immune regulators.

In addition to transcriptional regulation, analysis of the *TBF1* mRNA through the 5′ and 3′ rapid amplification of cDNA ends (RACE) detected two additional upstream open reading frames (uORFs) 5′ of the *TBF1* start codon (Figure 4C). The second uORF (At4g36988) is well-conserved among *TBF1* homologs in other plant species [25]. To test whether these two uORFs influence translation initiation of TBF1, we made a fusion between the 5′ UTR of *TBF1* containing both *uORFs*, the first exon of *TBF1* and the *GUS* reporter (abbreviated as *uORF1-uORF2-GUS*). We also created three additional constructs with the start codon mutated (ATG to CTG) for uORF1 (*uorf1-uORF2-GUS*), uORF2 (*uORF1-uorf2-GUS*), or both uORFs (*uorf1-uorf2-GUS*). These reporter constructs were driven by the 35S promoter to allow detection of only translational differences. We first transiently expressed these constructs in *Nicotiana benthamiana* leaves and quantified the GUS activities (Figure 4D). Using activity of the WT construct as a control, we detected 1.5- and 3.5-fold increases in GUS activities in *uorf1-uORF2-GUS* and *uORF1-uorf2-GUS*, respectively. Like the *uorf2* mutant, mutating both uORFs in *uorf1-uorf2-GUS* resulted in a 3.5-fold elevation in GUS activity over WT. These observations suggest that both uORFs have inhibitory effects on TBF1 translation, with the effect of uORF2 epistatic to that of uORF1.

To further understand the regulatory mechanism of TBF1 translation during plant defense, we quantified GUS activities of these translational fusions in stable transgenic *Arabidopsis* lines in response to *Psm* ES4326 carrying the avirulent effector, avrRpt2. We found that perception of this avirulent bacterial strain, which can induce MTI, ETI, and SAR, caused a rapid increase in GUS activity in the *uORF1-uORF2-GUS* transgenic lines (Figure 4E). Interestingly, this increase was not observed in the *uorf1-uorf2-GUS* transgenic lines. These results suggest that the *Psm* ES4326/avrRpt2 challenge could rapidly alleviate the inhibitory effects of the uORFs on translation of the downstream gene. To determine whether the endogenous TBF1 was indeed translated in the plant cell upon pathogen challenge, we conducted a polysome profiling experiment (Figure 4F). We found a significant increase in *TBF1* transcript in the polysomal fractions of the gradient within 30 min of *Psm* ES4326/avrRpt2 inoculation (Figure 4G), consistent with the results from the study using the GUS reporter (Figure 4E). Moreover, this polysomal association appeared to be transient as the *TBF1* transcript decreased 1 hr post inoculation. In contrast, polysomal association of the housekeeping gene *UBQ5* transcript was not significantly increased upon pathogen challenge (Figure S4).

Both uORFs of TBF1 are enriched in aromatic amino acids, particularly in phenylalanine (Phe). Intriguingly, this Phe enrichment is evolutionarily conserved for uORF2 among the TBF1 homologs in other plant species [25]. We hypothesize that pathogen challenge may result in a decrease in cellular Phe concentration and allow translation initiation of TBF1 downstream of uORFs.

Because repeated efforts in measuring Phe concentrations in plants infected with *Psm* ES4326/avrRpt2 have not produced consistent results, we employed a yeast-based reporter system (see Experimental Procedures). This system involves the use of the yeast strain *aro7*, which is auxotrophic for Phe and tyrosine, and the reporter containing the mouse DHFR (dihydrofolate reductase), which has been engineered to be less stable [26] and resistant to methotrexate (MTX) [27]. In the presence of MTX, yeast growth becomes dependent on the recombinant DHFR reporter expression. We inserted *uORF1-uORF2-TBF1*$^{1st\ exon}$ upstream of the *DHFR* reporter to generate *uORF1-uORF2-DHFR* and transformed this construct into *aro7*. The resulting transformant was cultured in the presence of MTX and growth was recorded over the course of time.

As shown in Figure 5A, under the Phe-rich conditions (75 mg/L; standard Phe concentration), the yeast strain carrying the *DHFR* displayed a much higher growth rate than

the strain carrying the *uORF1-uORF2-DHFR*, showing the inhibitory effects of the *uORF*s on DHFR translation. However, under the Phe-restricting conditions (15 mg/L), both strains grew at similar rates, suggesting that low Phe level released the inhibitory effects of uORFs on DHFR translation (Figure 5A). To ensure that the TBF1$^{1st\ exon}$ –DHFR fusion protein was not toxic to yeast cells, we grew the strains in the absence of MTX and noted no significant difference in their growth (Figure S5). The uORFs of TBF1 appear to be specifically sensitive to Phe starvation because aspartic acid (Asp) starvation caused by addition of tobramycin (TOB), a known inhibitor of yeast tRNA^{Asp} aspartylation [28], did not eliminate the difference in growth rate between the strain carrying *uORF1-uORF2-DHFR* and the strain carrying DHFR.

We next sought to understand how Phe starvation alleviates uORFs-mediated repression of TBF1 translation. In yeast, amino acid starvation results in a series of events including uncharged tRNAs accumulation, activation, and autophosphorylation of GCN2, GCN2-mediated phosphorylation of eukaryotic initiation factor 2α (eIF2α), and translation initiation of GCN4 downstream of uORFs [29–32]. To determine whether a similar mechanism controls the translation of TBF1, we first performed northern blot analysis to measure charged and uncharged tRNA levels following inoculation with *Psm* ES4326/avrRpt2. We detected a dramatic increase in both charged and uncharged tRNA^{Phe} within 30 min of the bacterial inoculation, which persisted for 8 hr (Figure 5B). In contrast, only a moderate increase in charged tRNA^{Asp} level was observed under the same conditions. No uncharged tRNA^{Asp} was detected. This is consistent with our hypothesis that pathogen challenge in plants can lead to specific changes in Phe metabolism.

Because a functional and stress-inducible GCN2-eIF2α pathway has been found in *Arabidopsis* [33], we investigated whether the pathogen-induced accumulation of uncharged tRNA^{Phe} could lead to phosphorylation of eIF2α. In an immunoblot experiment, we detected a rapid accumulation of the phosphorylated eIF2α in *Arabidopsis* leaves infected with *Psm* ES4326/avrRpt2 (Figure 5C). The phosphorylated eIF2α may facilitate ribosome reattachment to the TBF1 translation start codon downstream of uORFs to initiate TBF1 translation.

Taken together, we concluded that TBF1 expression is tightly controlled not only at the transcriptional level by NPR1 but also at the translational level through uORFs. Pathogen challenge, which causes a temporary increase in uncharged tRNA^{Phe} accumulation, triggers eIF2α phosphorylation and consequently derepression of TBF1 translation.

Discussion

The presence of *TL1* in a wide array of defense-related gene promoters (Figures 2D and 2E) [3, 34, 35] suggests a critical role for its binding TF in plant immune responses. Consistent with these genomic data, we demonstrated that the *tbf1* mutant plants are impaired in UPR, elf18-induced MTI and SA-mediated SAR, but not in the heat-shock response (Figure 3; Figure S3B). Evolution of such TFs with novel functions may explain the greater number of HSF-like genes in plants than in other organisms (one each in yeast and *Drosophila*, three in vertebrates) [36].

Activation of the immune system requires significant metabolic activities. It is well known that mutant plants with constitutively activated defense response often have stunted growth and retarded development [37]. Our study demonstrates that in response to MTI and SAR induction, TBF1 is a master molecular switch for the growth-to-defense reprogramming that involves activation and repression of nearly 3,000 genes, of which 46% contain at least one

copy of the *TL1* element in their promoters. TBF1 controls not only immune response genes but also genes involved in growth and development.

The pivotal role that TBF1 plays in the growth-to-defense transition underlines the importance of understanding its regulation. TBF1 expression is tightly controlled at both transcriptional and translational levels. Transcription of TBF1 and NPR1 appears to be interdependent because mutation of either gene affects transcription of the other (Figures 4A and 4B). TBF1 may directly regulate *NPR1* expression through the *TL1* elements in the *NPR1* promoter. Because the *NPR1* promoter also contains W-boxes [38], it is also possible that TBF1 regulates NPR1 indirectly through its transcriptional targets, WRKY TFs (Table S1). Reciprocally, NPR1 may regulate *TBF1* expression through either WRKY or TGA TFs because the *TBF1* promoter contains five W-boxes and three TGA binding sites known as the *as-1* elements [39].

The two uORFs of TBF1 link its translation with cellular amino acid availability. Approximately 10% of eukaryotic mRNA contain uORFs, and a high percentage of them encode critical cellular regulators: protooncogenes, TFs, receptors, and proteins involved in immune responses [40]. Expression of such genes is highly regulated, because their protein products are essential for controlled cell growth and proliferation. Indeed, TBF1 is such a regulator as transgenic lines overexpressing the TBF1 cDNA under the constitutive 35S promoter were not viable (K.M.P.-M. and X.D., unpublished data).

Pathogen challenge and the subsequent increase in uncharged $tRNA^{Phe}$ and phosphorylation of eIF2α release the inhibitory effects of uORFs on TBF1 translation (Figure 5D). This is reminiscent of the regulatory mechanism described for the well-studied yeast GCN4 and mammalian ATF4 (reviewed in [32]). The yeast *GCN4* transcript contains four uORFs in its 5′ region [41]. Under normal conditions, ribosomes bind to the 5′ cap of *GCN4* mRNA and initiate translation of the first uORF. They are unable to reinitiate translation at the start codon of GCN4. During amino-acid starvation, uncharged tRNAs induce phosphorylation of eIF2α mediated by GCN2, which hinders reassembly of the 80S ribosome after translation of uORF1. This allows the 40S ribosomal subunit to continue scanning the mRNA and reinitiate translation at the start codon of GCN4 [41].

Whereas derepression of GCN4 translation can be triggered by starvation of any amino acid, uORF-mediated regulation of TBF1 in plants appears to be controlled by the metabolism of specific amino acids, such as Phe. It is uncertain whether pathogen infection causes a transient starvation of Phe. The rapid increase in the uncharged $tRNA^{Phe}$ after pathogen challenge coincided with an increase of the total $tRNA^{Phe}$ suggesting that the accumulation of uncharged $tRNA^{Phe}$ may result from decreased availability of Phe as well as increased $tRNA^{Phe}$ synthesis (Figure 5B). However, it is tempting to hypothesize that pathogen infection affects Phe availability for translation because aromatic amino acids are known precursors for a large array of plant metabolites such as the growth hormone auxin, the SAR signal SA, cell wall components, and pigments such as anthocyanins [4, 42, 43]. Similar to GCN4, the accumulation of uncharged $tRNA^{Phe}$ triggers phosphorylation of eIF2α, ribosomal movement through uORFs, and translation of TBF1. The translation regulatory mechanism of TBF1 allows the cell to quickly detect pathogen-triggered metabolic changes and produce the TBF1 protein to activate immune responses. Our data suggest that plants employ TBF1 in response to infection to rapidly reprogram cellular transcription, which diverts energy resources to cope with pathogens at the expense of growth and development (Figure 5D).

Experimental Procedures

Translational Analysis of uORF1-uORF2-GUS

The DNA fragment containing the 5′UTR and the first exon of *TBF1* (designated *uORF1-uORF2*) was PCR amplified using primers TBF1 5′UTR-GW-F and TBF1 5′UTR-GW-R (Table S3) and cloned into the Gateway vector pDONR207 (Invitrogen). Two A-to-C point mutations were introduced, either separately or together, into the start codons (ATG) of *uORF1* and *uORF2*. The WT and mutant *uORF1-uORF2* sequences were inserted downstream of the constitutive 35S promoter and upstream of the coding region of the *GUS* reporter in pMDC140 through recombination [44]. The resulting translational reporters were transformed into *Col-0* WT plants or transiently expressed in *Nicotiana benthamiana* using *Agrobacterium tumefaciens* [45]. For *Arabidopsis* stable transgenic lines, two independent T_3 lines homozygous for each construct were chosen for quantitative GUS assay [3] at 0, 0.5, 1, 2, 3, 4, and 8 hr after *Psm* ES4326/avrRpt2 infiltration (OD_{600nm} = 0.02). Further detailed experimental procedures are described in the Supplemental Information.

Supplementary Material

Refer to Web version on PubMed Central for supplementary material.

Acknowledgments

We thank N. Spivey for sharing microarray data, D. Thiele and D. Neef for performing *TBF1* complementation assay in yeast *hsf1* mutant, C. Nicchitta for assistance in the polysome profiling experiment, T. Pan for input in the tRNA study, M. Froneberger for helping with the experiments, and J. Siedow and S. Mukhtar for critical reading of the manuscript and helpful discussions. This project was supported by a grant from the National Science Foundation (MCB-0519898) to X.D., Grants-in-Aid for Scientific Research (No. 23120520) from the Ministry of Education, Culture, Sports, Science and Technology of Japan to Y.T., and the Hargitt Fellowship to K.M.P.-M. X.D. is a Howard Hughes Medical Institute – Gordon and Betty Moore Foundation investigator.

References

1. Nishimura MT, Dangl JL. Arabidopsis and the plant immune system. Plant J. 2010; 61:1053–1066. [PubMed: 20409278]
2. Jones JD, Dangl JL. The plant immune system. Nature. 2006; 444:323–329. [PubMed: 17108957]
3. Wang D, Weaver ND, Kesarwani M, Dong X. Induction of protein secretory pathway is required for systemic acquired resistance. Science. 2005; 308:1036–1040. [PubMed: 15890886]
4. Durrant WE, Dong X. Systemic acquired resistance. Annu Rev Phytopathol. 2004; 42:185–209. [PubMed: 15283665]
5. Kwon C, Bednarek P, Schulze-Lefert P. Secretory pathways in plant immune responses. Plant Physiol. 2008; 147:1575–1583. [PubMed: 18678749]
6. Nekrasov V, Li J, Batoux M, Roux M, Chu ZH, Lacombe S, Rougon A, Bittel P, Kiss-Papp M, Chinchilla D, et al. Control of the pattern-recognition receptor EFR by an ER protein complex in plant immunity. EMBO J. 2009; 28:3428–3438. [PubMed: 19763086]
7. Saijo Y, Tintor N, Lu X, Rauf P, Pajerowska-Mukhtar K, Häweker H, Dong X, Robatzek S, Schulze-Lefert P. Receptor quality control in the endoplasmic reticulum for plant innate immunity. EMBO J. 2009; 28:3439–3449. [PubMed: 19763087]
8. Kinkema M, Fan W, Dong X. Nuclear localization of NPR1 is required for activation of *PR* gene expression. Plant Cell. 2000; 12:2339–2350. [PubMed: 11148282]
9. Song J, Durrant WE, Wang S, Yan S, Tan EH, Dong X. DNA repair proteins are directly involved in regulation of gene expression during plant immune response. Cell Host Microbe. 2011; 9:115–124. [PubMed: 21320694]
10. Zhang Y, Fan W, Kinkema M, Li X, Dong X. Interaction of NPR1 with basic leucine zipper protein transcription factors that bind sequences required for salicylic acid induction of the *PR-1* gene. Proc Natl Acad Sci USA. 1999; 96:6523–6528. [PubMed: 10339621]

11. Kotak S, Larkindale J, Lee U, von Koskull-Döring P, Vierling E, Scharf KD. Complexity of the heat stress response in plants. Curr Opin Plant Biol. 2007; 10:310–316. [PubMed: 17482504]
12. Baniwal SK, Bharti K, Chan KY, Fauth M, Ganguli A, Kotak S, Mishra SK, Nover L, Port M, Scharf KD, et al. Heat stress response in plants: a complex game with chaperones and more than twenty heat stress transcription factors. J Biosci. 2004; 29:471–487. [PubMed: 15625403]
13. Boscheinen O, Lyck R, Queitsch C, Treuter E, Zimarino V, Scharf KD. Heat stress transcription factors from tomato can functionally replace HSF1 in the yeast Saccharomyces cerevisiae. Mol Gen Genet. 1997; 255:322–331. [PubMed: 9268023]
14. Busch W, Wunderlich M, Schöffl F. Identification of novel heat shock factor-dependent genes and biochemical pathways in Arabidopsis thaliana. Plant J. 2005; 41:1–14. [PubMed: 15610345]
15. Prändl R, Hinderhofer K, Eggers-Schumacher G, Schöffl F. HSF3, a new heat shock factor from Arabidopsis thaliana, derepresses the heat shock response and confers thermotolerance when overexpressed in transgenic plants. Mol Gen Genet. 1998; 258:269–278. [PubMed: 9645433]
16. Czarnecka-Verner E, Pan S, Salem T, Gurley WB. Plant class B HSFs inhibit transcription and exhibit affinity for TFIIB and TBP. Plant Mol Biol. 2004; 56:57–75. [PubMed: 15604728]
17. Czarnecka-Verner E, Yuan CX, Scharf KD, Englich G, Gurley WB. Plants contain a novel multi-member class of heat shock factors without transcriptional activator potential. Plant Mol Biol. 2000; 43:459–471. [PubMed: 11052198]
18. Panstruga R, Parker JE, Schulze-Lefert P. SnapShot: Plant immune response pathways. Cell. 2009; 136:978. [PubMed: 19269372]
19. Sugano S, Jiang CJ, Miyazawa S, Masumoto C, Yazawa K, Hayashi N, Shimono M, Nakayama A, Miyao M, Takatsuji H. Role of OsNPR1 in rice defense program as revealed by genome-wide expression analysis. Plant Mol Biol. 2010; 74:549–562. [PubMed: 20924648]
20. Kumar M, Busch W, Birke H, Kemmerling B, Nürnberger T, Schöffl F. Heat shock factors HsfB1 and HsfB2b are involved in the regulation of Pdf1.2 expression and pathogen resistance in Arabidopsis. Mol Plant. 2009; 2:152–165. [PubMed: 19529832]
21. Zipfel C, Kunze G, Chinchilla D, Caniard A, Jones JD, Boller T, Felix G. Perception of the bacterial PAMP EF-Tu by the receptor EFR restricts Agrobacterium-mediated transformation. Cell. 2006; 125:749–760. [PubMed: 16713565]
22. Li J, Zhao-Hui C, Batoux M, Nekrasov V, Roux M, Chinchilla D, Zipfel C, Jones JD. Specific ER quality control components required for biogenesis of the plant innate immune receptor EFR. Proc Natl Acad Sci USA. 2009; 106:15973–15978. [PubMed: 19717464]
23. Lu X, Tintor N, Mentzel T, Kombrink E, Boller T, Robatzek S, Schulze-Lefert P, Saijo Y. Uncoupling of sustained MAMP receptor signaling from early outputs in an Arabidopsis endoplasmic reticulum glucosidase II allele. Proc Natl Acad Sci USA. 2009; 106:22522–22527. [PubMed: 20007779]
24. Tsuda K, Sato M, Stoddard T, Glazebrook J, Katagiri F. Network properties of robust immunity in plants. PLoS Genet. 2009; 5:e1000772. [PubMed: 20011122]
25. Hayden CA, Jorgensen RA. Identification of novel conserved peptide uORF homology groups in Arabidopsis and rice reveals ancient eukaryotic origin of select groups and preferential association with transcription factor-encoding genes. BMC Biol. 2007; 5:32. [PubMed: 17663791]
26. Tucker CL, Fields S. A yeast sensor of ligand binding. Nat Biotechnol. 2001; 19:1042–1046. [PubMed: 11689849]
27. Ercikan-Abali EA, Waltham MC, Dicker AP, Schweitzer BI, Gritsman H, Banerjee D, Bertino JR. Variants of human dihydrofolate reductase with substitutions at leucine-22: effect on catalytic and inhibitor binding properties. Mol Pharmacol. 1996; 49:430–437. [PubMed: 8643082]
28. Walter F, Pütz J, Giegé R, Westhof E. Binding of tobramycin leads to conformational changes in yeast tRNA(Asp) and inhibition of aminoacylation. EMBO J. 2002; 21:760–768. [PubMed: 11847123]
29. Dey M, Cao C, Sicheri F, Dever TE. Conserved intermolecular salt bridge required for activation of protein kinases PKR, GCN2, and PERK. J Biol Chem. 2007; 282:6653–6660. [PubMed: 17202131]

30. Dong J, Qiu H, Garcia-Barrio M, Anderson J, Hinnebusch AG. Uncharged tRNA activates GCN2 by displacing the protein kinase moiety from a bipartite tRNA-binding domain. Mol Cell. 2000; 6:269–279. [PubMed: 10983975]

31. Padyana AK, Qiu H, Roll-Mecak A, Hinnebusch AG, Burley SK. Structural basis for autoinhibition and mutational activation of eukaryotic initiation factor 2alpha protein kinase GCN2. J Biol Chem. 2005; 280:29289–29299. [PubMed: 15964839]

32. Hinnebusch AG. Translational regulation of GCN4 and the general amino acid control of yeast. Annu Rev Microbiol. 2005; 59:407–450. [PubMed: 16153175]

33. Lageix S, Lanet E, Pouch-Pélissier MN, Espagnol MC, Robaglia C, Deragon JM, Pélissier T. Arabidopsis eIF2alpha kinase GCN2 is essential for growth in stress conditions and is activated by wounding. BMC Plant Biol. 2008; 8:134. [PubMed: 19108716]

34. Fabro G, Di Rienzo JA, Voigt CA, Savchenko T, Dehesh K, Somerville S, Alvarez ME. Genome-wide expression profiling Arabidopsis at the stage of Golovinomyces cichoracearum haustorium formation. Plant Physiol. 2008; 146:1421–1439. [PubMed: 18218973]

35. Humphry M, Bednarek P, Kemmerling B, Koh S, Stein M, Göbel U, Stüber K, Pislewska-Bednarek M, Loraine A, Schulze-Lefert P, et al. A regulon conserved in monocot and dicot plants defines a functional module in antifungal plant immunity. Proc Natl Acad Sci USA. 2010; 107:21896–21901. [PubMed: 21098265]

36. Nover L, Bharti K, Döring P, Mishra SK, Ganguli A, Scharf KD. Arabidopsis and the heat stress transcription factor world: how many heat stress transcription factors do we need? Cell Stress Chaperones. 2001; 6:177–189. [PubMed: 11599559]

37. Heidel AJ, Clarke JD, Antonovics J, Dong X. Fitness costs of mutations affecting the systemic acquired resistance pathway in Arabidopsis thaliana. Genetics. 2004; 168:2197–2206. [PubMed: 15611186]

38. Eulgem T, Rushton PJ, Robatzek S, Somssich IE. The WRKY superfamily of plant transcription factors. Trends Plant Sci. 2000; 5:199–206. [PubMed: 10785665]

39. Lebel E, Heifetz P, Thorne L, Uknes S, Ryals J, Ward E. Functional analysis of regulatory sequences controlling PR-1 gene expression in Arabidopsis. Plant J. 1998; 16:223–233. [PubMed: 9839467]

40. Kozak M. An analysis of vertebrate mRNA sequences: intimations of translational control. J Cell Biol. 1991; 115:887–903. [PubMed: 1955461]

41. Miller PF, Hinnebusch AG. cis-acting sequences involved in the translational control of GCN4 expression. Biochim Biophys Acta. 1990; 1050:151–154. [PubMed: 2207139]

42. Holton TA, Cornish EC. Genetics and Biochemistry of Anthocyanin Biosynthesis. Plant Cell. 1995; 7:1071–1083. [PubMed: 12242398]

43. Zhao Y. Auxin biosynthesis and its role in plant development. Annu Rev Plant Biol. 2010; 61:49–64. [PubMed: 20192736]

44. Curtis MD, Grossniklaus U. A gateway cloning vector set for high-throughput functional analysis of genes in planta. Plant Physiol. 2003; 133:462–469. [PubMed: 14555774]

45. Pajerowska-Mukhtar KM, Mukhtar MS, Guex N, Halim VA, Rosahl S, Somssich IE, Gebhardt C. Natural variation of potato allene oxide synthase 2 causes differential levels of jasmonates and pathogen resistance in Arabidopsis. Planta. 2008; 228:293–306. [PubMed: 18431595]

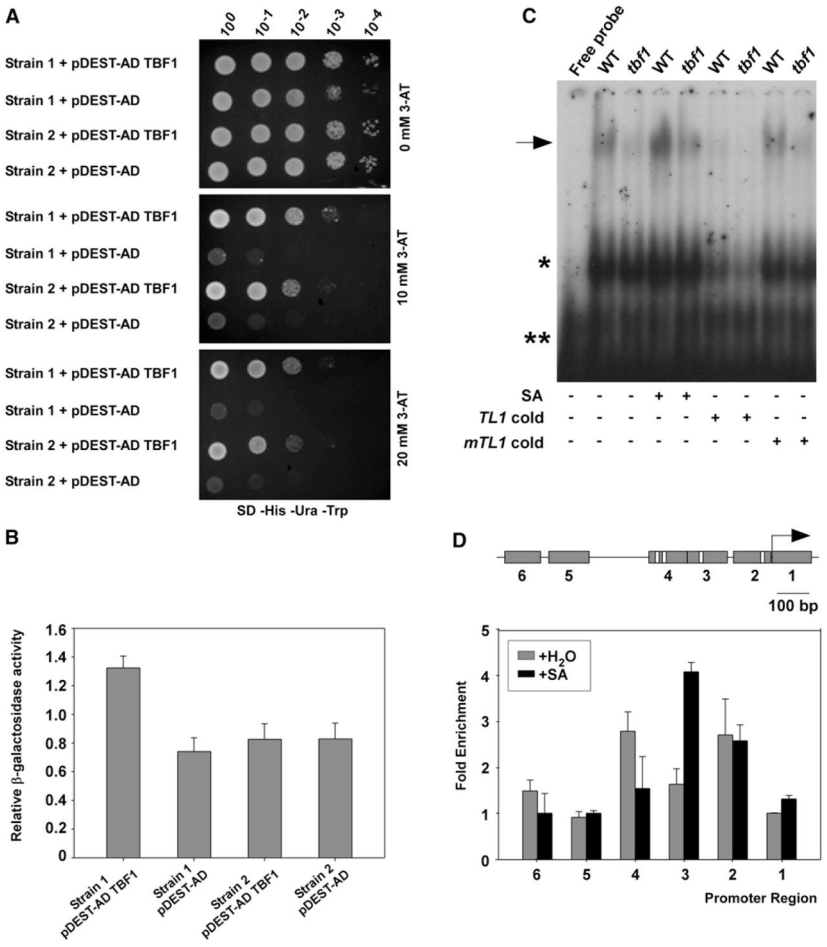

Figure 1. HSF4 Is the *TL1*-Binding TF, TBF1

(A and B) TBF1 (HSF4) binding to the *TL1 cis* elements in the *BiP2* promoter was detected in Y1H. Yeast growth on selective media (SD-His-Ura-Trp) supplemented with increasing concentrations of 3-AT was recorded at day 3 (A). β-galactosidase reporter activity was measured using ONPG as the substrate (B). Error bars represent standard deviation from three different technical replications. Both (A) and (B) were repeated three times with similar results. See also Figures S1A and S1B.

(C) Electrophoretic mobility shift assay was performed using plant extracts from WT and the *tbf1* mutant upon 1 mM SA treatment. *TL1* cold and *mTL1* cold (mutant *TL1*; both at 5 pmol/μL) were used as unlabeled probes. The arrow marks the TBF-*TL1* complex. Asterisks indicate nonspecific binding. (+) and (−) signify for the presence or absence of corresponding treatments. The experiment was repeated three times with similar results. See also Figures S1Cand S1D.

(D) TBF1-GFP binding to the *TL1* elements in the *BiP2* promoter was measured by ChIP after treatment with H_2O or 1mMSA. The PCR amplicons, 1 to 6 (gray boxes) with *TL1* elements highlighted in white are shown (upper panel). Arrow represents the BiP2 translational start site. Normalized fold enrichment for each amplicon was calculated (lower panel). Error bars represent standard deviation from three different replicates. Experiment was repeated five times with similar results. See also Figure S1E.

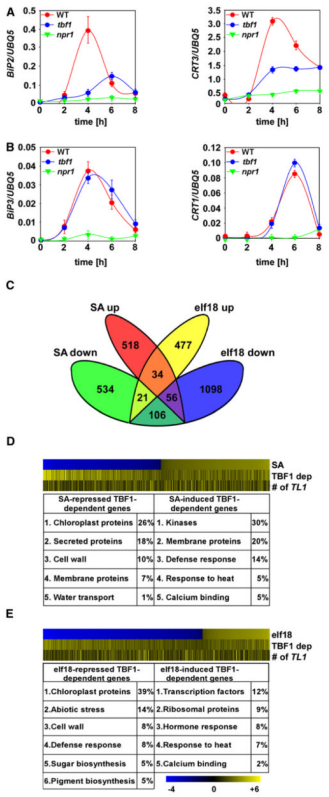

Figure 2. TBF1 Plays aMajor Role in Transcriptional Reprogramming during MTI and SAR

(A and B) Relative transcript levels of TBF1-dependent and independent ER-resident genes were determined by qRT-PCR using cDNA generated from WT, *tbf1*, and *npr1-1* plants treated with 1mMSA. Error bars represent standard deviation from nine technical replicates derived from three independent experiments. See also Figure S2A.

(C) Venn diagram shows the numbers of TBF1-dependent SA downregulated (SA down), SA upregulated (SA up), elf18 upregulated (elf18 up), and elf18 downregulated (elf18 down) genes ($p < 0.05$).

(D and E) Heat maps of TBF1-regulated genes in total numbers (top), degrees of TBF1 dependency (middle), and numbers of *TL1 cis* elements in the gene promoters (bottom) in response to SA (D) and elf18 (E) treatment. Top ranked functional groups were determined using DAVID Gene Ontology. Scale indicates the log-transformed p values of down-(blue) and up-(yellow) regulated genes (top), yellow lines indicate TBF1 dependency (middle), and yellow lines correspond to the numbers of *TL1 cis* elements in the gene promoters (bottom). See also Figures S2B–S2E.

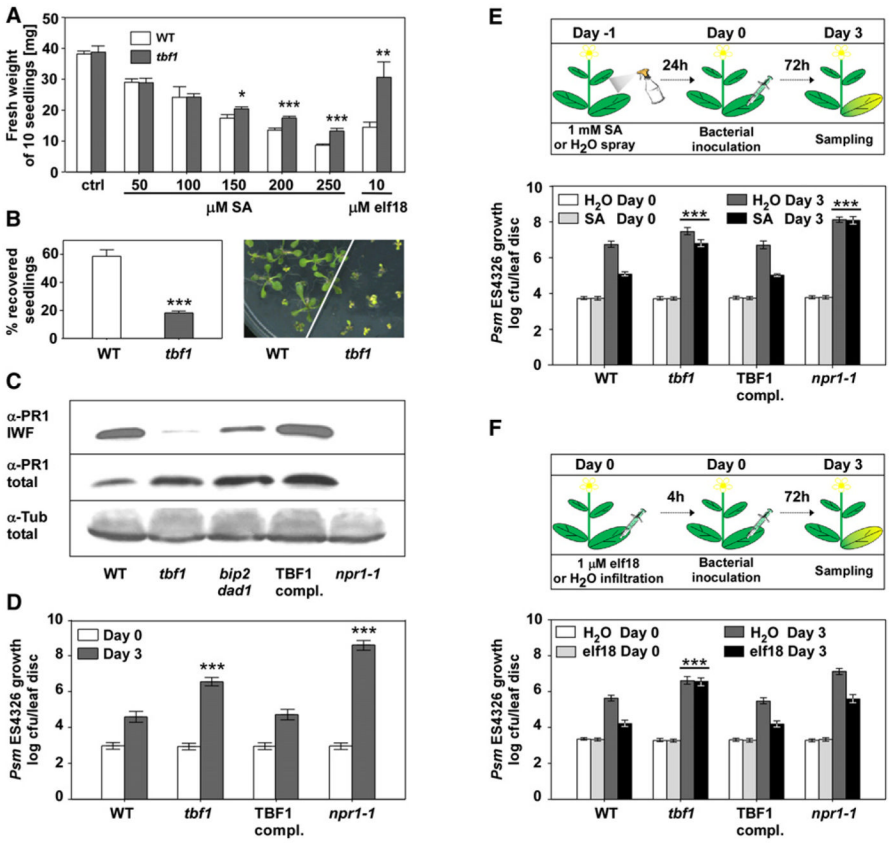

Figure 3. TBF1 Is a Major Molecular Switch for the Growth-to-Defense Transition

(A) Fresh weight of ten seedlings grown for 10 days on plates with MS growth media (ctrl), or MS supplemented with increasing concentrations of SA or 10 µM elf18. Error bars represent standard deviation of three replicates. This experiment was repeated three times with similar results. Statistical analysis was performed using Student's t test, *$p < 0.05$, **$p < 0.01$, ***$p \leq 0.001$. See also Figure S3A.

(B) Seedling recovery after treatment with tunicamycin was measured by counting the percentage of surviving seedlings (left) and by phenotype observations (right). Error bars represent standard deviation of three replicates. This experiment was repeated five times with similar results. Statistical analysis was performed using Student's t test, ***$p \leq 0.001$. See also Figure S3B.

(C) PR1 accumulation in the intercellular wash fluid (IWF) and total protein extracts from leaves of 3-week-old WT, *tbf1, tbf1* transformed with the WT *TBF1* gene (TBF1 compl.), *npr1-1*, and *bip2 dad2*. For loading controls, an antibody against tubulin (α-Tub) was used to probe the total protein blot. See also Figure S3C.

(D) Enhanced disease susceptibility was measured in 3-week-old WT, *tbf1*, TBF1 complementation, and *npr1-1* plants 3 days after infiltration with a bacterial suspension of *Psm* ES4326 (OD_{600nm} = 0.0001). Error bars represent 95% confidence intervals of 24 replicates derived from three independent experiments. This experiment was repeated at least five times with similar results. Statistical analysis was performed using Bonferroni post hoc test, ***$p < 0.0001$.

(E) SA-induced resistance was determined according to the schematic representation (upper panel), and the growth of *Psm* ES4326 was plotted as in (D) but with a higher initial inoculum (OD_{600nm} = 0.001) (lower panel). Error bars represent 95% confidence intervals

of 24 replicates derived from three independent experiments. Statistical analysis was performed using two-way analysis of variance (ANOVA), ***$p < 0.0001$.
(F) elf18-induced resistance was measured according to the schematic representation (upper panel) and with the initial *Psm* ES4326 inoculum of $OD_{600nm} = 0.001$ (lower panel). Error bars represent 95% confidence intervals of 24 replicates derived from three independent experiments. Statistical analysis was performed using two-way ANOVA, ***$p < 0.0001$. See also Figures S3D and S3E.

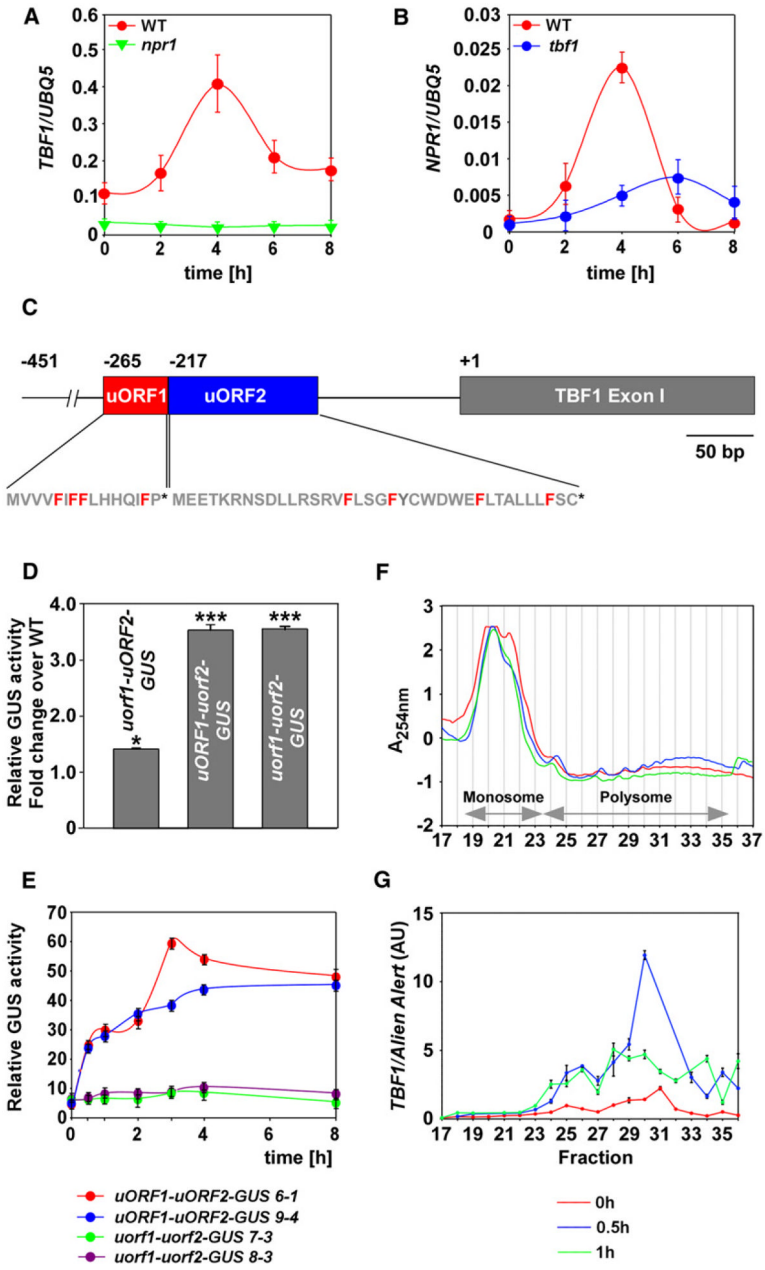

Figure 4. TBF1 Expression Is Regulated at both Transcriptional and Translational Levels

(A and B) Relative transcript levels of *TBF1* (A) and *NPR1* (B) genes in response to 1 mM SA treatment were determined by qRT-PCR. Error bars represent standard deviation from nine technical replicates derived from three independent experiments.

(C) Schematic representation of uORF1 and uORF2 and exon I of *TBF1*. The phenylalanines (F) in uORF1 and uORF2 are highlighted in red, and the stop codons are shown as asterisks. "+1" represents the translational start of TBF1 and −451, −265, and −217 represent the upstream positions of the 5′ end of the transcript, the start codon for uORF1, and the start codon for uORF2, respectively.

(D) Quantification of GUS activity in *Nicotiana benthamiana* leaves transiently expressing *uORF1-uORF2-GUS* (WT), *uorf1-uORF2-GUS*, *uORF1-uorf2-GUS*, and *uorf1-uorf2-GUS*. This experiment has been repeated three times with similar results.

(E) Quantification of translational inhibitory effect exerted by uORFs in transgenic T_3 plants expressing *uORF1-uORF2-GUS* (two independent transformants 6-1 and 9-4) or *uorf1-uorf2-GUS* (two independent transformants 7-3 and 8-3) at various time points after inoculation with *Psm* ES4326/avrRpt2 (OD_{600nm} = 0.02). Error bars represent standard deviation from three different replicates. Experiment was repeated at least three times with similar results.

(F and G) Polysome profiles (F) and *TBF1* expression (G) in samples obtained from WT plants at 0, 0.5, and 1 hr after inoculation with *Psm* ES4326/avrRpt2 (OD_{600nm} = 0.02). The fractions containing monosome and polysome were annotated based on the absorbance at 254 nm (A_{254nm}). The *TBF1* transcript abundance normalized against Alien Alert® control transcript is expressed in arbitrary units (AU). Error bars represent standard error. This experiment was repeated using two biological replicates (each with three technical replicates) with similar results. See also Figure S4.

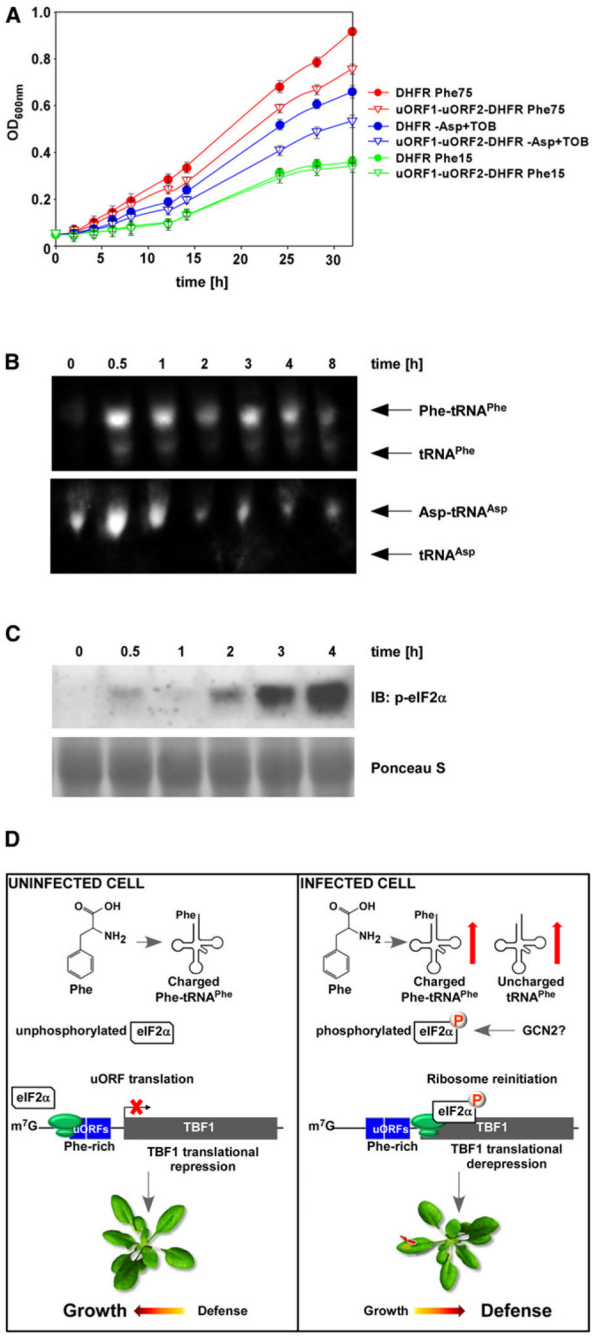

Figure 5. TBF1 Translation Is Regulated in Response to Pathogen-Induced Changes in Phenylalanine Metabolism

(A) The effects of phenylalanine and aspartate starvation on the translational inhibitory function of uORFs were measured by growth of the yeast strain *aro7* (phe^{-}, tyr^{-}) transformed with the *uORF1-uORF2-DHFR* or *DHFR* reporter in medium containing methotrexate, an inhibitor of the endogenous DHFR. Optical densities for cultures containing two different concentrations of phenylalanine (Phe; 15 and 75 mg/L) as well as cultures lacking Asp and supplemented with tobramycin (TOB), an inhibitor of yeast tRNA^{Asp} aspartylation, were recorded over the course of 32 hr. Error bars represent standard

deviation from nine technical replicates derived from three independent experiments. See also Figure S5.

(B) tRNA analysis of WT plants at various time points after inoculation with *Psm* ES4326/avrRpt2 (OD_{600nm} = 0.02). Northern blot using probes against $tRNA^{Phe}$ or $tRNA^{Asp}$ was performed to detect charged and uncharged $tRNA^{Phe}$ or $tRNA^{Asp}$. This experiment was repeated using three biological replicates with similar results.

(C) Phosphorylated form of eIF2α was detected using a phospho-specific antibody in the total protein extracts from leaves of 3-week-old WT plants collected at various time points after inoculation with *Psm* ES4326/avrRpt2 (OD_{600nm} = 0.02). Ponceau S stain was used to determine equal loading.

(D) A model illustrating the molecular mechanism by which the translation initiation of TBF1 is regulated through rapid increases in uncharged and charged $tRNA^{Phe}$, phosphorylation of eIF2α, and ribosomal read-through of uORFs, leading to the growth-to-development transition.